INTERNATIONAL JOURNAL OF CLIMATOLOGY
Int. J. Climatol. **35**: 1858–1866 (2015)
Published online 21 July 2014 in Wiley Online Library
(wileyonlinelibrary.com) DOI: 10.1002/joc.4093

RMetS
Royal Meteorological Society

Simulating direct effects of dust aerosol on arid and semi-arid regions using an aerosol–climate coupled system

Shuyun Zhao,[a,b,c] Hua Zhang,[c]* Song Feng[d] and Qiang Fu[e]

[a] *Chinese Academy of Meteorological Sciences, Beijing, China*
[b] *University of Chinese Academy of Sciences, Beijing, China*
[c] *Laboratory for Climate Studies, National Climate Center, China Meteorological Administration, Beijing, China*
[d] *Department of Geosciences, University of Arkansas, Fayetteville, AR, USA*
[e] *Department of Atmospheric Sciences, University of Washington, Seattle, Washington, DC, USA*

ABSTRACT: This work uses an aerosol–climate coupled system to study the direct climatic effects of dust aerosol on global arid (including hyper-arid) and semi-arid regions. Results show that dust aerosol can cause surface cooling over these regions. The cooling effects of dust aerosol are larger in the Northern Hemisphere (NH) than in the Southern Hemisphere (SH). This asymmetric cooling leads to a severer reduction in evaporation over the low latitudes of the NH compared with their counterpart areas in the SH. In addition, air descent is enhanced (or ascent is weakened) by dust aerosol over the low latitudes of the NH, whereas the reverse happens in the SH. With the anomalous in evaporation and circulation, precipitation is decreased (increased) over the arid and semi-arid areas in the NH (SH) by dust aerosol. Dust aerosol can decrease the potential evapotranspiration in arid and semi-arid regions mainly by decreasing the net radiation flux at the top of the atmosphere, which compensates for the decrease in precipitation caused by dust aerosol. Therefore, as the dominant aerosol in the arid and semi-arid regions, dust aerosol does not exacerbate the aridity over most of these regions. The effects of dust aerosol are indiscernible in the expansion of arid and semi-arid areas on a global scale.

KEY WORDS dust aerosol; arid and semi-arid; AGCM

Received 3 July 2013; Revised 3 March 2014; Accepted 28 May 2014

1. Introduction

Dust aerosol, as an abundant type of aerosol in the atmosphere, can scatter and absorb solar and terrestrial radiation, influencing the regional and global climate (Foster *et al.*, 2007). Miller *et al.* (2004) pointed out that dust aerosol could reduce global evaporation and precipitation by reducing surface temperature, but overall acts as a negative feedback to desertification. Through its effect on atmospheric circulation, dust aerosol can also influence the activity of monsoon. For instance, Lau *et al.* (2006) and Lau and Kim (2006) suggested that the absorption of elevated dust aerosol accompanied with black carbon led to an earlier onset and intensification of the Indian Monsoon, through an 'elevated heating pump' mechanism. This 'elevated heating pump' mechanism of dust aerosol also enhanced the West African Monsoon in boreal summer, leading to an increase of rainfall over the West Africa/Eastern Atlantic inter-tropical convergence zone (ITCZ) and a decrease of rainfall over the Western Atlantic and Caribbean regions (Lau *et al.*, 2009). Zhao *et al.* (2012) found that dust aerosol from Western America may cause an eastward migration of moisture convergence driven by North America Monsoon and a sequent increase in precipitation over Arizona-New Mexico-Texas regions.

Some studies specially investigated the impact of dust aerosol on arid and semi-arid regions, where surface is bare or poorly vegetated (Islam and Almazroui, 2012; Sun *et al.*, 2012). Since dust aerosol originated mainly in these regions (Marticorena and Bergametti, 1995; Zender *et al.*, 2003), it might exert more influence on the climate in these regions than in other regions. Arid (including hyper-arid) and semi-arid areas account for about one-third of the earth's land surface and are an important part of the earth's major ecosystems (Reynolds *et al.*, 2007). Owing to excessive grazing/deforestation (Schlesinger *et al.*, 1990), ecosystems over these regions are vulnerable and sensitive to climate changes (Emanuel *et al.*, 1985). Islam and Almazroui (2012) suggested that dust aerosol might increase the wet season precipitation in Arabian Peninsula based on the simulation of ICTP-RegCM4. Using the same model as Islam and Almazroui (2012), Sun *et al.* (2012) suggested that dust aerosol tends to increase summer precipitation around its source areas but suppress summer precipitation in its downward areas in East Asia. However, the study of dust aerosol on the climate change in the arid and semi-arid regions is still rare, and most previous studies are focused on its climatic effects over a specific arid or semi-arid region. No attempts have been made to investigate the effects of dust aerosol on arid and

* Correspondence to: H. Zhang, Laboratory for Climate Studies, National Climate Center, China Meteorological Administration, Beijing 100081, China. E-mail: huazhang@cma.gov.cn.

semi-arid areas over the entire globe, as well as their effects on the aridity and areal extent of arid and semi-arid regions.

By using an aerosol-climate coupled system BCC_AGCM2.0.1_CAM (Zhang *et al.*, 2012), this study evaluated the effects of dust aerosol on arid and semi-arid regions by examining their direct interaction with radiation from a global perspective. Special attention was paid to the influence of dust aerosol on the aridity and spatial distribution of arid and semi-arid areas, by examining the anomaly in aridity index (AI; UNEP, 1992) induced by dust aerosol. The UNEP (1992) AI was defined as the ratio of precipitation to potential evapotranspiration (PET), which is a quantitative indicator of the degree of water scarcity at a given region. Thus, gaining knowledge on the changes in aridity may lead to better understanding of the impact of climate change and human activities on arid and semi-arid regions.

This article is organized as follows. Models and model experiments as well as the methods to define arid and semi-arid areas are described in Section 2. Changes in temperature, precipitation, and aridity caused by dust aerosol over arid and semi-arid regions are investigated in Section 3, followed by conclusions and discussion in Section 4.

2. Models and methods

2.1. Models and model experiments

We use the general circulation model developed at the National Climate Centre of the Chinese Meteorological Administration (BCC_AGCM2.0.1; Wu *et al.*, 2010). The model is based on Community Atmospheric Model version 3.0 from the National Centre for Atmospheric Research (NCAR). The model was further developed to be coupled online with the Canadian Aerosol Model (CAM; Gong *et al.*, 2002, 2003a), with updated aerosol emission sources (Zhou *et al.*, 2012), as described by Zhang *et al.* (2012). In addition, a new method of Monte Carlo Independent column approximation (McICA) dealing with the cloud overlapping was introduced by Jing and Zhang (2012) and Zhang *et al.* (2014), and the radiation scheme BCC-RAD developed by Zhang *et al.* (2003a, 2006a, 2006b) was adopted.

The CAM is a size-segregated aerosol model that includes the processes for the emission, transport, chemical transformation, cloud interaction, and deposition of five typical aerosols, sulfate, black carbon, organic carbon, dust, and sea salt. The radii of aerosols fall into 12 bins: 0.005-0.01, 0.01-0.02, 0.02-0.04, 0.04-0.08, 0.08-0.16, 0.16-0.32, 0.32-0.64, 0.64-1.28, 1.28-2.56, 2.56-5.12, 5.12-10.24, and 10.24-20.48 μm. The emission data were primarily from AeroCom, which includes the surface emission rate of black and organic carbon (Bond *et al.*, 2004; Van der Werf *et al.*, 2004), SO_2 and sulfate (Van der Werf *et al.*, 2004; Cofala *et al.*, 2005), and DMS (Kettle and Andreae, 2000; Nightingale *et al.*, 2000). Other emission data were from the Emission Database for Global Atmospheric Research (EDGAR) version 3.2, 1995, database (Olivier *et al.*, 2002; http://www.mnp.nl/edgar). The sea-salt module was developed by Gong *et al.* (2002). An online sulfur chemistry module was included in CAM, in which H_2S, DMS, SO_2, and H_2SO_4 are prognostic variables, whereas OH, O_3, H_2O_2, and NO_3 are prescribed offline from the MOZART/NCAR model (Brasseur *et al.*, 1998; Hauglustaine *et al.*, 1998). The soil dust emission scheme was developed by Marticorena and Bergametti (1995), in which the surface velocity and roughness were the main factors that determined the vertical flux of dust aerosol. Three lognormal population distributions for dust in China were used, and the mass median diameters and standard deviations of these three populations were determined by considering the soil features in China and source region dust size-distribution measurements (Gong *et al.*, 2003b; Zhang *et al.*, 2003b). Out of China, the two-mode size distribution for dust from the observation by Chatenet *et al.* (1996) was used.

To couple aerosols with atmospheric radiative processes, the optical properties of the aerosols (e.g. extinction coefficient, single scattering *albedo*, and asymmetry parameter) were calculated according to the band division of the BCC-RAD based on Mie theory. The refractive indices of dry aerosols were adopted from D'Almeida *et al.* (1991), and the Mie scattering code of Wiscombe (1980) was used. The effects of water vapour on the size distributions and optical properties of three hygroscopic aerosols, sulfate, organic carbon, and sea salt, have been considered. In this study, 10 relative humidities were considered: 0.0, 0.45, 0.5, 0.6, 0.7, 0.8, 0.9, 0.95, 0.98, and 0.99. In the calculations, first, the radii of the 12-size bins of wet particles for each relative humidity were obtained. The effective refractive indices of the wet particles were then computed using a volume-weighted method. The optical properties of the aerosols were obtained for the 12-size bins with 10 relative humidities in 17 spectral bands, and these properties were used to form the look-up tables (Wei and Zhang, 2011; Wang *et al.*, 2013). The optical properties of the aerosols for any relative humidity could therefore be easily obtained using linear interpolation in the climate model. It has been noted that the non-sphericity of dust aerosols has little effect on their radiative forcing (Fu *et al.*, 2009; Wang *et al.*, 2013), and the optical properties can therefore be derived from the Mie theory.

The aerosol–climate coupled system BCC_AGCM2.0.1 _CAM was run for 50 years with and without considering the radiative effect of dust aerosol, named RUN + DUST and RUN-DUST for short, respectively. To examine the interaction between dust aerosol and the global climate, a slab ocean model (Hansen *et al.*, 1984) was coupled in both runs. The horizontal resolution of the model was set at T42 ($\sim 2.8 \times 2.8°$), with 26 vertical layers on the hybrid σ-pressure coordinate. All other model parameters in both experiments were identical, meaning that any differences between the two experiments are a result of the impact of dust aerosol on the simulated climate.

In this study, we analysed the model results of the past 30 years using the first 20 years as the spin-up data. It is important to evaluate a model's capacity before using it to perform studies. The evaluation focusing on the capability

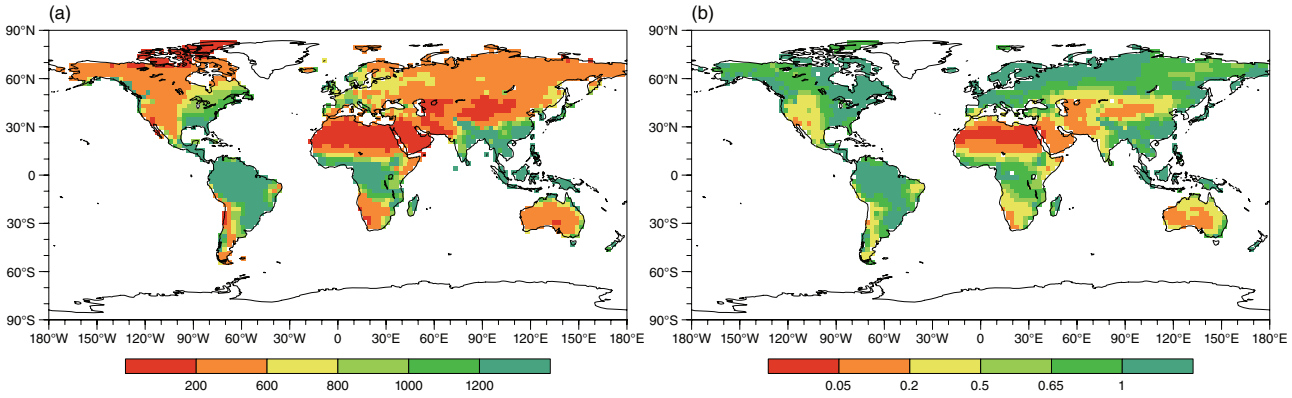

Figure 1. Global distributions of (a) calibrated annual mean precipitation (unit: mm yr^{-1}) and (b) aridity index, based on the model calibrated results of RUN + DUST (unit: 1).

of BCC_AGCM2.0.1 to reproduce meteorological fields had been given in detail by Wu *et al.* (2010), whereas the evaluation focusing on the capability of the model to reproduce the dust aerosol had been given in detail by Zhang *et al.* (2012), Wang *et al.* (2013), and Zhao *et al.* (2014).

2.2. Definitions of the arid and semi-arid areas

The areal extent of the arid and semi-arid areas must be identified before examining the effects of dust aerosol on these regions. Different criteria have been used to define arid and semi-arid regions, including annual precipitation (Huang *et al.*, 2012) and a combination of annual precipitation and PET (UNEP, 1992; Feng and Fu, 2013). The criteria based on merely precipitation are simple and may reasonably define the arid and semi-arid areas in the middle and low latitudes (e.g. Sahara Desert, Arabian Peninsula, and Western Australia). The precipitation criteria, however, also classify the higher latitudes (north of 50°N) as arid and semi-arid (Figure 1(a)), which is inconsistent with Koppen–Geiger climate classification (Kottek *et al.*, 2006; Feng *et al.*, 2014)

This study defines the arid and semi-arid regions using the (AI (UNEP, 1992), which is based on the ratio between the annual mean precipitation (P) and annual mean PET. The global land surface can be classified as hyper-arid ($AI < 0.05$), arid ($0.05 \le AI < 0.2$), semi-arid ($0.2 \le AI < 0.5$), dry sub-humid ($0.5 \le AI < 0.65$), sub-humid ($0.65 \le AI < 1$), or humid ($AI \ge 1$). In this article, PET is calculated using the Penman–Monteith method, as described in the Food and Agriculture Organization (FAO) Irrigation and Drainage Paper (Allen *et al.*, 1998). The Penman–Monteith method simultaneously accounts for the effects of radiation, temperature, wind speed, and humidity:

$$PET = \frac{0.408\Delta\left(R_n - G\right) + \gamma\frac{900}{T+273}u_2\left(e_s - e_a\right)}{\Delta + \gamma\left(1 + 0.34u_2\right)} \quad (1)$$

where R_n is the net radiation at the surface (MJ m^{-2} day^{-1}); G, the soil heat flux density (MJ m^{-2} day^{-1}); T, the air temperature at 2-m height (°C); u_2, the wind speed at 2-m height (m s^{-1}); e_s and e_a are the saturation and actual vapour pressure, respectively (kPa); Δ, the slope vapour-pressure curve (kPa °C^{-1}); and γ, a psychrometric constant (kPa °C^{-1}). Figure 1(b) indicates the wide distribution of arid (including hyper-arid) and semi-arid areas around the world. Large arid and semi-arid regions appear in North Africa, the Arabian Peninsula, Central Asia, Northwestern China, Southwest North America, and central and Western Australia. Arid and semi-arid regions are also seen over the west Namibia and South Africa, and highlands in the eastern and southern parts of South America. Most areas north of 50°N in Figure 1(b) are classified as sub-humid and humid regions, suggesting a more realistic classification using AI than just using annual precipitation.

3. Climate effects of dust aerosol on arid and semi-arid areas

As shown in Figure 2(a), higher dust aerosol burden is distributed in the tropical and sub-tropical regions in both hemispheres, with peaks in arid and semi-arid areas and their downwind regions. The simulated total burden of dust aerosol in the atmosphere is 30.8 Tg, which is slightly larger than the simulations from the Goddard Institute for Space Sciences (GISS) model (29.0 Tg) and the Goddard Global Ozone Chemistry Aerosol Radiation and Transport (GOCART) model (29.5 Tg) (Huneeus *et al.*, 2011). These differences are likely because only the GISS and GOCART models consider dust aerosol with diameter smaller than 10 μm, whereas our model considers dust aerosol smaller than 20.48 μm. Of the total content of atmospheric dust aerosol, more than 90% is located in the Northern Hemisphere, which is mostly attributed to the dust emission from the Sahara Desert. The climate effects of this asymmetric distribution of dust aerosol about the equator will be discussed in the following sections. Dust aerosol can reduce the net incoming radiation flux at the top of atmosphere (TOA) because it reflects solar radiation, leading to a decrease in surface temperature. The total effect of dust aerosol on the net radiation flux (shortwave + longwave) at the TOA is

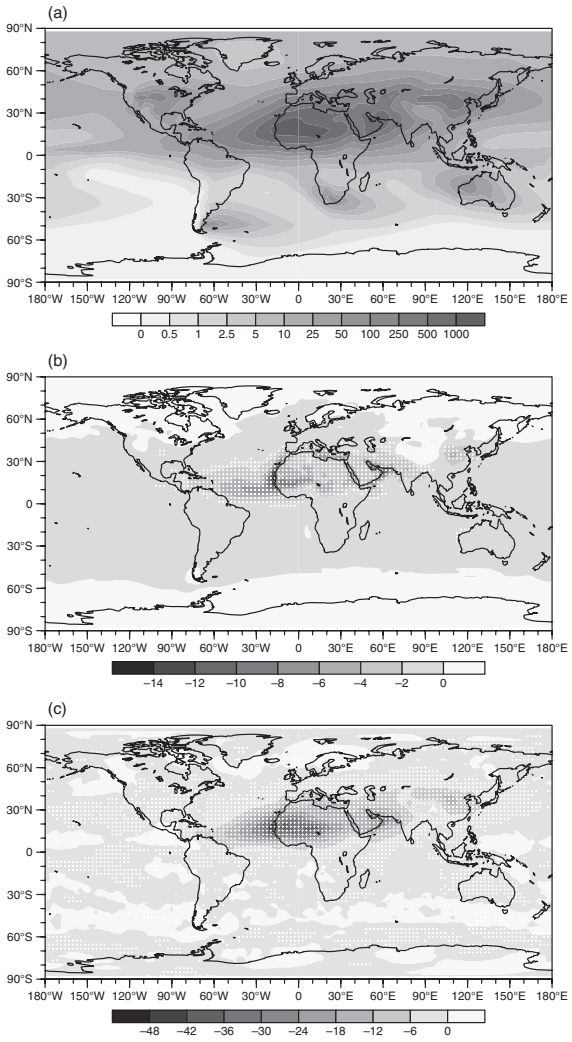

Figure 2. Distributions of (a) the column burden of dust aerosol (unit: mg m^{-2}), (b) the effects of dust aerosol on the net radiation (shortwave + longwave) at the TOA (unit: W m^{-2}), and (c) the effects of dust aerosol on the net radiation (shortwave + longwave) at the surface. White dots indicates results below the significance cutoff of 0.05.

shown in Figure 2(b). The dust aerosol can reduce incoming radiation energy in most terrestrial areas, especially over arid and semi-arid areas and their downward regions. The global average effect of dust aerosol on the net radiation at the TOA is −0.62 (−0.68 ∼ −0.56) W m^{-2}, and −2.83 (−3.01 ∼ −2.65) W m^{-2} at the surface, respectively. The value at the TOA is slightly larger than the adjusted radiative forcing from spherical dust aerosol calculated by Wang *et al.* (2013), which used the same model configuration as in this study but used a fixed sea surface temperature instead of the slab ocean model.

3.1. Temperature

The radiative effects of dust aerosol lead to a global decrease in surface temperature (Figure 3(a)), except for a small portion of the Northern Europe and Central America. The cooling effect is especially pronounced in the arid and semi-arid areas such as Sahara Desert, where dust aerosol can cool the surface temperature by up to 4 K. The changes in surface temperature in most areas can be explained by the direct radiative effects of dust aerosol. Dust aerosol can absorb and scatter shortwave radiation, leading to the reduction of solar radiation reaching the surface and consequently causing surface cooling. A few exceptions (e.g. the Central America) suggest that cloud feedback to aerosol direct effect may be important in the coastal regions of the tropics.

The surface cooling induced by dust aerosol varies seasonally (Figure 4, left panel). In North China, dry and windy springs are in favour of dust emission and transportation. The decrease of surface temperature over this area and its downwind areas in spring is more obvious than in other seasons (Figure 4(b)). The extensive cooling around Arabian Peninsula in summer (Figure 4(c)) is consistent with the main dry season mainly from June to September in this area (Islam and Almazroui, 2012). In Sahara region, the band of temperature decrease shifts north in summer and south in winter (Figure 4(a) and (c)), mainly relate to the match of the subtropical high. The change of surface temperature caused by dust aerosol is −0.503 K in boreal summer and −0.475 K in winter, and the values for spring and fall are in the between.

3.2. Precipitation

Compared to temperature, the response of precipitation to dust aerosol is more inhomogeneous (Figure 3(b) and Figure 4, right panel), suggesting that the effects of dust aerosol on precipitation are more complex. On a global

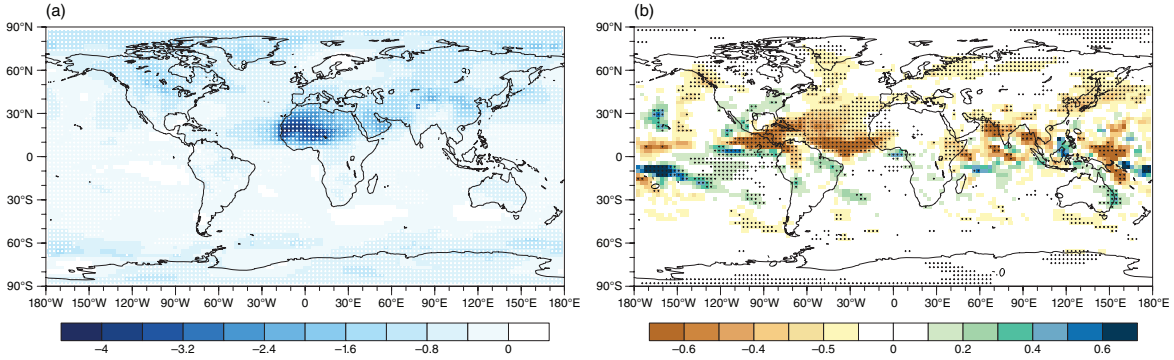

Figure 3. Changes in (a) annual mean surface temperature (unit: K) and (b) annual mean precipitation (unit: mm day^{-1}) caused by soil dust, with white dots and black dots indicating results below the significance cutoff of 0.05.

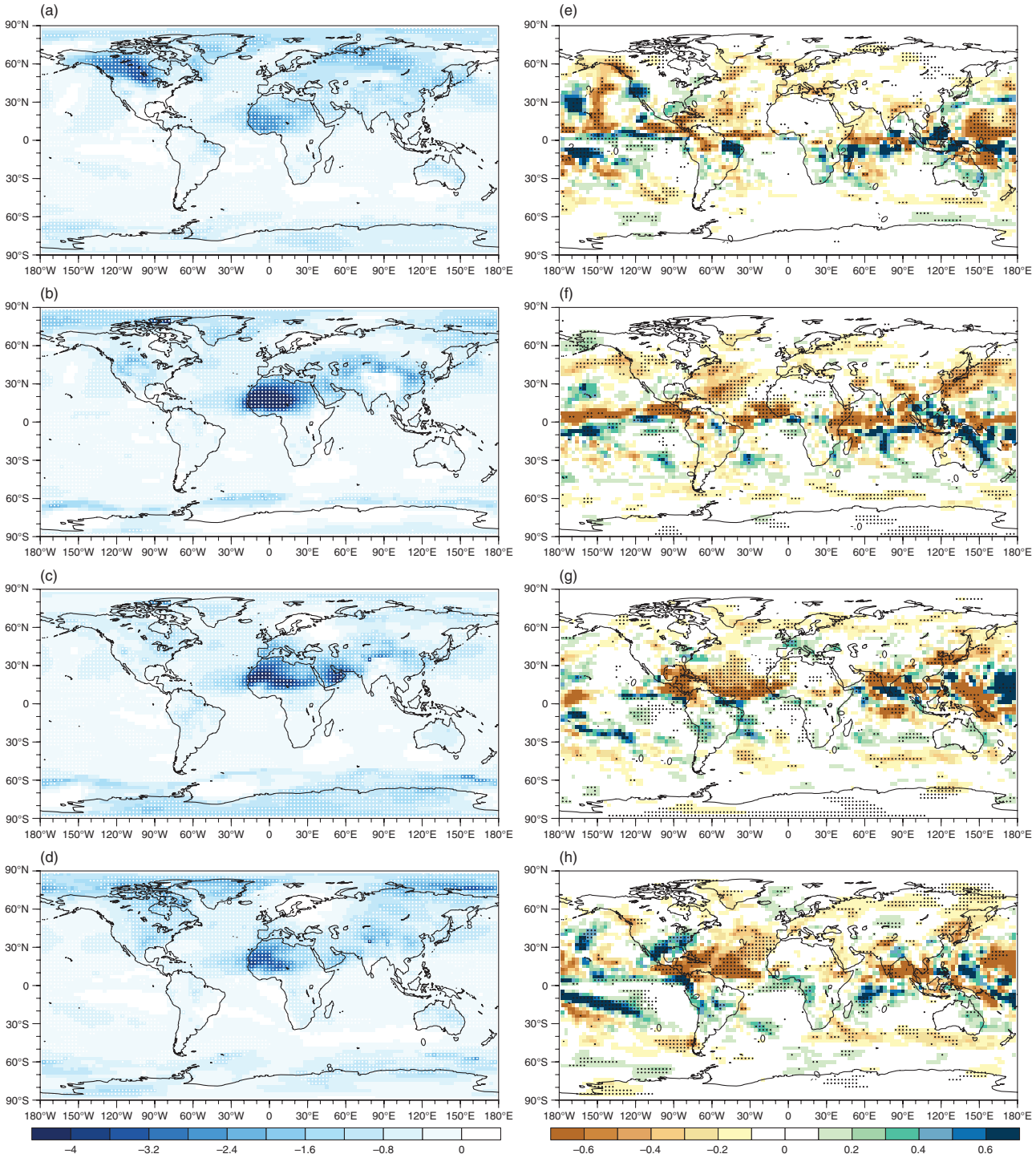

Figure 4. Anomalies in (left panel) seasonal mean surface temperature (unit: K) and (right panel) seasonal mean precipitation (unit: mm day^{-1}) induced by dust aerosol, with white dots and black dots indicating results below the significant cutoff of 0.05. (a) and (e) for December to February (DJF), (b) and (f) for March to May (MAM), (c) and (g) for June to August (JJA), and (d) and (h) for September to November (SON).

average, the simulated change of rainfall induced by dust aerosol is −0.075 mm day^{-1} and −0.061 mm day^{-1} in boreal spring and summer, respectively. The values for winter and fall are slightly larger than −0.05 mm day^{-1}.

Over arid and semi-arid areas, where the effects of dust aerosol are much more important than over the rest of the terrestrial regions, dust aerosol may either suppress (e.g. the Sahara Desert) or enhance the precipitation (e.g. central and Western Australia). In general, the annual precipitation is decreased in most parts of the arid and semi-arid areas in the Northern Hemisphere, whereas is increased in the Southern Hemisphere (Figure 3(b)).

Compared with the cooling in the tropical Southern Hemisphere, there is much stronger surface cooling in the lower latitudes of the Northern Hemisphere, which induces a strong northward temperature gradient

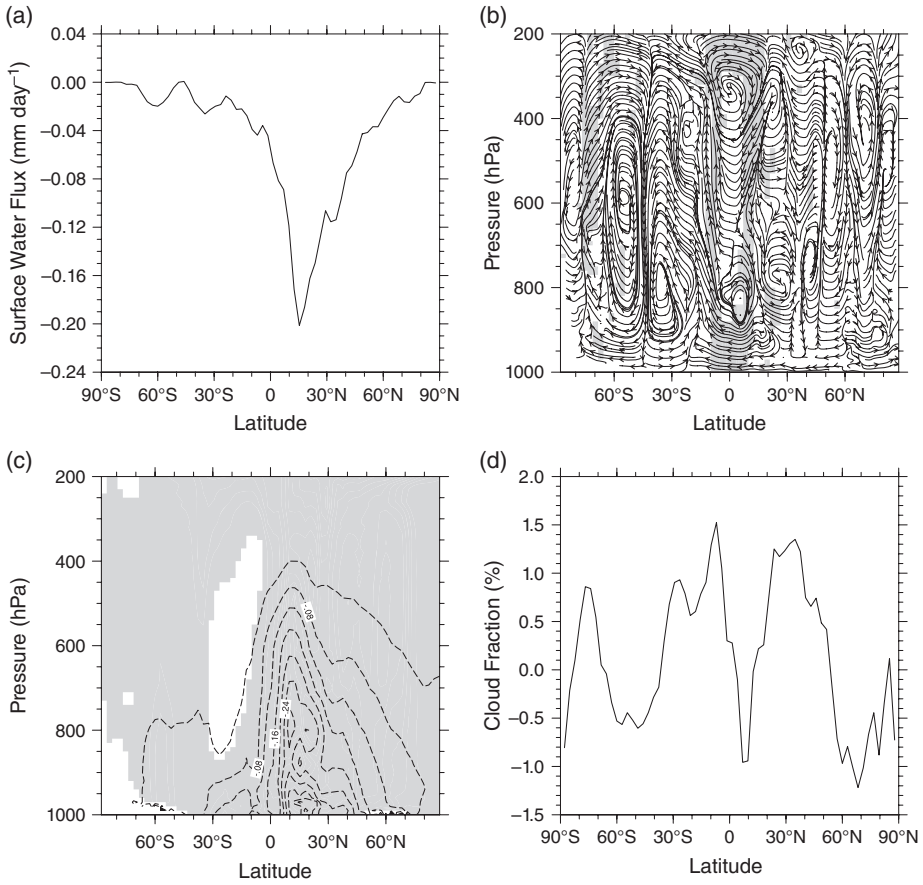

Figure 5. Changes in (a) evaporation (mm day^{-1}), (b) meridional circulation, (c) specific humidity (g kg^{-1}) and (d) (high + median + low) cloud fraction (unit: %) caused by dust aerosol, with shaded areas (b and c) indicating levels below the significance cutoff of 0.05.

(Figure 3(a)). This is mainly caused by the asymmetric distribution of dust aerosol about the equator (Figure 1(b) and Figure 2(a)). Correspondingly, the evaporation is reduced most severely over the low latitude areas of the Northern Hemisphere than elsewhere (Figure 5(a)), with a zonal mean reduction up to about 0.20 mm day^{-1} between 10°N and 20°N. Owing to the heterogeneous change in surface temperature, there is a northerly trend of wind in the lower atmospheric levels, whereas a southerly trend of wind in the upper atmospheric levels, between 30°S and 30°N. In addition, air tends to ascend more strongly (or descend more weakly) in the Southern Hemisphere near 30°S and tends to descend more strongly (or ascend more weakly) in the Northern Hemisphere near 30°N, suggesting that dust aerosol can enhance the general circulation in the Northern hemisphere and weaken it in the Southern Hemisphere.

With these anomalous in evaporation and circulation, a strong reduction in specific humidity is observed between 30°N and the equator than elsewhere (Figure 5(c)). In the low levels of tropical Northern Hemisphere, the zonal mean specific humidity is reduced as much as 0.4 g kg^{-1}. The northward gradient of specific humidity is enhanced by dust aerosol above the equatorial area. It can be seen in Figure 5(d) that the cloud is inhibited over the low latitudes of the Northern Hemisphere and enhanced over the low latitudes of the Southern Hemisphere. The change in precipitation (Figure 3(b)) is consistent with that in cloud fraction (Figure 5(d)).

In general, the enhanced cooling over the Northern Hemisphere caused by the abundant dust aerosol load can not only depress the evaporation, but also inhibit the cloud. The humidity and dynamical conditions are not in favour of the formation of precipitation over the low latitudes of the Northern Hemisphere. Over the low latitudes of the Southern Hemisphere, the changes in evaporation and humidity are relatively small (Figure 5(a) and (d)), but the weakened air descent facilitates cloud development and precipitation. These responses of precipitation to the asymmetric change of temperature about the equator are consistent with the findings of Broccoli *et al.* (2006) and Wang *et al.* (2013).

3.3. Aridity and areal extent of arid and semi-arid regions

Dust aerosol leads to increased AI (reduced aridity) over the middle of Sahara Desert, Northwestern China and Central Asia, West North America, and most arid and semi-arid areas in the Southern Hemisphere (Figure 6). However, AI is decreased (increased aridity) over the west and east coasts of North Africa, the Arabian Peninsula, and the highlands from Iran to North India. Changes in AI can be caused by the changes in precipitation and/or the PET.

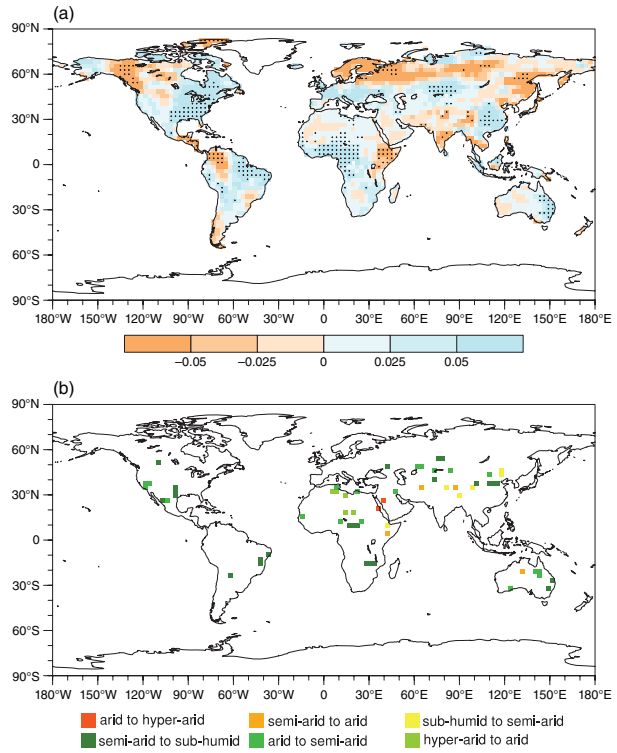

Figure 6. Changes in (a) AI, with dots indicating results below the significance level of 0.05 and (b) areas of arid and semi-arid regions (AI < 0.5) by dust aerosol radiative effects. Different colours in (b) show the change in areal extent of the arid and semi-arid regions caused by dust aerosol.

The change in AI can be written as follows:

$$\Delta AI_{\mathrm{U}} = \frac{P}{PET}\left(\frac{1}{P}\Delta P - \frac{1}{PET}\Delta PET\right) \qquad (2)$$

The above-mentioned equation clearly suggests that the change in AI is dependent on the relative changes in P and PET. Taking the middle of Sahara Desert as an example, dust aerosol suppresses precipitation (Figure 3(b)) by inhibiting vertical movement and cools the surface, lessening the water demand (i.e. decreasing the PET, Figure 7), causing a collective increase in AI and a reduction in aridity (Figure 6(a)). Similar changes in precipitation, PET, and AI can be found over the Northwestern China and Central Asia. However, in western North America and the most arid and semi-arid areas in the Southern Hemisphere, the change in precipitation and PET both favour increased AI. Overall, dust aerosol does not lead to the expansion of the total areal extent of the earth's arid and semi-arid areas. Dust aerosol may reduce the hyper-arid areas in the north of Africa and arid and semi-arid areas in western North America, Central Asia, northwestern China, and Australia (Figure 6(b)). However, it is worth noting that dust aerosol may degrade some arid places on both sides of the Red Sea into hyper-arid areas and enlarge arid and semi-arid areas in some parts of northern and western China and the Somalia Peninsula.

Similar results are found when classifying arid and semiarid region using the Koppen–Geiger climate classification (not shown), which suggests that our results

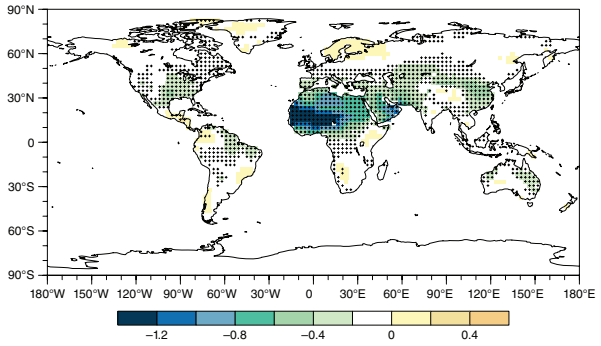

Figure 7. Change in PET caused by dust aerosol, with dots indicating results below the significance level of 0.05; unit: mm day^{-1}.

are robust. Although dust aerosol neither exacerbates the dryness over arid and semi-arid areas nor leads to the global expansion of arid and semi-arid areas, the effort towards anti-desertification is not useless. Dust aerosol can cause high latitudes to become drier (Fig. 6a). In addition, dust aerosol can work as cloud condensation nuclei and change the global microphysics of clouds and climate (Rosenfeld *et al.*, 2001; IPCC, Foster *et al.*, 2007). Because of these effects, controlling the process of desertification is an urgent task for climate scientists.

PET is an important variable to quantify the potential water requirement for crops. As discussed previously, changes in PET play an important role in causing changes in AI in some places. The changes in PET caused by dust aerosol are shown in Figure 7. PET is reduced in most parts of arid and semi-arid areas, except for some small patches such as the east coast of North Africa. The global average change in PET is −0.230 mm day^{-1}.

The change in PET is controlled by surface temperature, net radiation, humidity, and wind speed, as described in Allen *et al.*, 1998. To quantitatively understand how dust aerosol may impact PET, we recalculated PET with one specific variable from the RUN + DUST and the other variables from the RUN-DUST. The difference between this recalculated PET and the original PET from the RUN-DUST is regarded as the contribution of the specific variable to the total change in PET caused by dust aerosol. The average 30 model years' annual and global mean contributions of these variables are shown in Table 1. Clearly, the total change in PET is not a linear combination of the contributions of surface temperature, net radiation flux, humidity, and wind on a global scale. In addition, the effects of dust aerosol on PET are primarily determined by the changes in net radiation, to a lesser extent by changes in the surface temperature and relative humidity, and least by changes in the surface wind.

4. Conclusion

The climate effects of dust aerosol on arid and semi-arid areas were evaluated using the aerosol–climate coupled system BCC_AGCM2.0.1_CAM. The arid and semi-arid regions were defined according to the criteria by UNEP (1992).

Table 1. Global average PET (unit: mm day^{-1}) and PET changing one variable at a time and keeping other variables the same.

Changing variables	Change of PET
Surface temperature	−0.079
Net radiation flux on the surface	−0.114
Relative humidity	−0.068
Surface wind	−0.018
Total	−0.280

Mainly due to its extinction of shortwave radiation, dust aerosol leads to surface cooling, especially over arid and semi-arid areas. However, the asymmetric distribution of dust aerosol about the equator has different effects on precipitation over arid and semi-arid areas in the two hemispheres, through its different effects on evaporation and general circulation, between 30°S and 30°N. Dust aerosol can either alleviate or exacerbate the dryness over some arid and semi-arid areas, depending on the comparative importance of its effects on precipitation and PET. As a net effect, dust aerosol does not enlarge the areal extent of arid and semi-arid regions on a global scale.

Dust aerosol both influences and responds to climate change. This work may provide some additional information about the role of dust aerosol on the climate change. However, this study only considered the direct effects of dust aerosol. Additional work is still needed to evaluate the indirect climate effects of dust aerosol. And the effects of anthropogenic aerosols on arid and semi-arid areas should be investigated in future work.

Acknowledgements

This work was financially supported by the National Basic Research Programme of China (2012CB955303 and 2011CB403405).

References

Allen RG, Pereira LS, Raes D, Smith M. 1998. Crop Evapotranspiration-Guidelines for Computing *Crop water Requirements-FAO Irrigation and Drainage Paper 56*. FAO, Rome, Retrieved July 9, 2014. http://www.fao.org/publications/card/en/c/5de3a877-5547-5b23-9e6f-0c8951c54b5e/.

Brasseur GP, Hauglustaine DA, Walters S, Rasch PJ, Muller JF, Granier C, Tie XX. 1998. MOZART, a global chemical transport model for ozone and related chemical tracers 1. Model description. *J. Geophys. Res.* **103**: 28265–28289.

Bond T, Streets D, Yarber K, Nelson S, Wo JH, Klimont Z. 2004. A technology-based global inventory of black and organic carbon emissions from combustion. *J. Geophys. Res.* **109**: D14203, DOI: 10.1029/2003JD003697.

Broccoli AJ, Dahl KA, Stouffer RJ. 2006. Response of the ITCZ to Northern Hemisphere cooling. *Geophys. Res. Lett.* **33**: L01702, DOI: 10.1029/2005GL024546.

Chatenet B, Marticorena B, Gomes L, Bergametti G. 1996. Assessing the size distribution of desert soils erodible by wind. *Sedimentology* **43**: 901–911.

Cofala J, Amann M, Klimont Z, Schopp W. 2005. Scenarios of world anthropogenic emissions of SO_2, NO_x and CO up to 2030. *Internal Report of the Transboundary Air Pollution Programme,* International Institute for Applied Systems Analysis, Laxenburg, Austria, 17 pp, Retrieved July 9, 2014. http://www.iiasa.ac.at/rains/global_emiss/global_emiss.html.

D'Almeida GA, Koepke P, Shettle EP. 1991. *Atmospheric Aerosols: Global Climatology and Radiative Characteristics*. Deepak Publishing: Hampton, VA.

Emanuel WR, Shugart HH, Stevenson MP. 1985. Climatic change and the broad-scale distribution of terrestrial ecosystem complexes. *Clim. Change* **7**(1): 29–43, DOI: 10.1007/BF00139439.

Foster P, Ramaswamy V, Artaxo P, Berntsen T, Betts R, Fahey DW, Haywood J, Lean J, Lowe DC, Myhre G, Nganga J, Prinn R, Raga G, Schulz M, Dorland RV. 2007. Changes in atmospheric constituents and in radiative forcing. *In Climate Change 2007: The Physical Science Basis. Contribution of Working Group I to the Fourth Assessment Report of the International Panel on Climate Change*, Solomon S, Qin D, Manning M, Chen Z, Marquis M, Averyt KB, Tignor M, Miller HL (eds). Cambridge University Press: Cambridge, UK and New York, NY.

Fu Q, Thorsen TJ, Su J, Ge JM, Huang JP. 2009. Test of Mie-based single-scattering properties of non-spherical dust aerosols in radiative flux calculations. *J. Quant. Spectrosc. Radiat. Transf.* **110**(14): 1640–1653, DOI: 10.1016/j.jqsrt.2009.03.010.

Feng S, Fu Q. 2013. Expansion of global drylands under a warming climate. *Atmos. Chem. Phys.* **13**: 14637–14665, DOI: 10.5194/acpd-13-14637-2013.

Feng S, Hu Q, Huang W, Ho CH, Li R, Tang Z. 2014. Projected climate regime shift under future global warming from multi-model multi-scenario CMIP5 simulations. *Glob. Planet. Chang.* **112**: 41–52.

Gong SL, Barrie LA, Lazare M. 2002. Canadian Aerosol Module (CAM): a size-segregated simulation of atmospheric aerosol processes for climate and air quality models 2. Global sea-salt aerosol and its budgets. *J. Geophys. Res.* **107**(D24): 4779, DOI: 10.1029/2001JD002004.

Gong SL, Barrie LA, Blanchet JP, von Salzen K, Lohmann U, Lesins G, Spacek L, Zhang LM, Girard E, Lin H, Leaitch R, Leighton H, Chylek P, Huang P. 2003a. Canadian Aerosol Module: a size-segregated simulation of atmospheric aerosol processes for climate and air quality models 1. Module development. *J. Geophys. Res.* **108**(D1): 4007, DOI: 10.1029/2001JD002002.

Gong SL, Zhang XY, Zhao TL, McKendry IG, Jaffe DA, Lu NM. 2003b. Characterization of soil dust aerosol in China and its transport and distribution during 2001 ACE-Asia: 2. Model simulation and validation. *J. Geophys. Res.* **108**(D9): 4262, DOI: 10.1029/2002JD002633.

Hansen J, Lacis A, Rind D, Russell G, Stone P, Fung I, Ruedy R, Lerner J. 1984. Climate sensitivity: analysis of feedback mechanisms. In *Climate processes and climate sensitivity, Geophysical Monograph Series 29*, Hansen JE, Takahashi T (eds). AGU: Washington, DC, 130–163, DOI: 10.1029/GM029p0130.

Hauglustaine DA, Brasseur GP, Walters S, Rasch PJ, Muller J-F, Emmons LK, Carroll MA. 1998. MOZART, a global chemical transport model for ozone and related chemical tracers 2. Model results and evaluation. *J. Geophys. Res.* **103**: 28291–28335.

Huang J, Guan X, Ji F. 2012. Enhanced cold-season warming in semi-arid regions. *Atmos. Chem. Phys.* **12**: 5391–5398, DOI: 10.5194/acp-12-5391-2012.

Huneeus N, Schulz M, Balkanski Y, Griesfeller J, Prospero J, Kinne S, Bauer S, Boucher O, Chin M, Dentener F, Diehl T, Easter R, Fillmore D, Ghan S, Ginoux P, Grini A, Horowitz L, Koch D, Krol MC, Landing W, Liu X, Mahowald N, Miller R, Morcrette JJ, Myhre G, Penner J, Perlwitz J, Stier P, Takemura T, Zender CS. 2011. Global dust model intercomparison in AeroCom phase I. *Atmos. Chem. Phys.* **11**: 7781–7816, DOI: 10.5194/acp-11-7781-2011.

Islam MN, Almazroui M. 2012. Direct effects and feedback of desert dust on the climate of the Arabian Peninsula during the wet season: a regional climate model study. *Clim. Dyn.* **39**: 2239–2250, DOI: 10.1007/s00382-012-1293-4.

Jing X, Zhang H. 2012. Application and evaluation of McICA cloud-radiation framework in the AGCM of the National Climate Center. *Chinese J. Atmos. Sci.* **36**(5): 945–958 (in Chinese).

Kettle AJ, Andreae MO. 2000. Flux of dimethysulfide from the oceans: a comparison of updated data sets and flux models. *J. Geophys. Res.* **105**: 26793–26808.

Kottek M, Grieser J, Beck C, Rudolf B, Rubel F. 2006. World map of the Köppen-Geiger climate classification updated. *Meteorol. Z.* **15**(3): 259–263.

Lau KM, Kim KM. 2006. Observational relationships between aerosol and Asian monsoon rainfall, and circulation. *Geophys. Res. Lett.* **33**: L21810, DOI: 10.1029/2006GL027546.

Lau KM, Kim MK, Kim KM. 2006. Asian summer monsoon anomalies induced by aerosol direct forcing: the role of the Tibetan Plateau. *Clim. Dyn.* **26**(7–8): 855–864, DOI: 10.1007/s00382-006-0114-z.

Lau KM, Kim KM, Sud YC, Walker GK. 2009. A GCM study of the response of the atmospheric water cycle of West Africa and the Atlantic to Sahara dust radiative forcing. *Ann. Geophys.* **27**: 4023–4037, DOI: 10.5194/angeo-27-4023-2009.

Marticorena B, Bergametti G. 1995. Modeling the atmospheric dust cycle: 1. Design of a soil-derived dust emission scheme. *J. Geophys. Res.* **100**(D8): 16415–16430, DOI: 10.1029/95JD00690.

Miller RL, Tegen I, Perlwitz J. 2004. Surface radiative forcing by soil dust aerosols and hydrologic cycle. *J. Geophys. Res.* **109**: D04203, DOI: 10.1029/2003JD004085.

Nightingale P, Malin G, Law C, Watson A, Liss P, Liddicoat M, Boutin J, Upstill-Goddard RC. 2000. In situ evaluation of air-sea gas exchange parameterizations using novel conservative and volatile tracers. *Glob. Biogeochem. Cycles* **14**: 373–387.

Olivier J, Berdowski J, Peters J, Bakker J, Visschedijk A, Bloos J. 2002. Applications of EDGAR including a description of ENDGAR V3.0: reference dataset with trend data for 1970-1995. NRP Report, 410200 051, RIVM, Bilthoven, the Netherlands.

Rosenfeld D, Rudich Y, Lahav R. 2001. Desert dust suppressing precipitation: a possible desertification feedback loop. *Proc. Natl. Acad. Sci. U. S. A.* **98**(11): 5975–5980, DOI: 10.1073/pnas.101122798.

Reynolds JF, Smith DMS, Lambin EF, Turner BL, Mortimore M, Batterbury SPJ, Downing TE, Dowlatabadi H, Fernández RJ, Herrick JE, Sannwald EH, Jiang H, Leemans R, Lynam T, Maestre FT, Ayarza M, Walker B. 2007. Global desertification: building a science for dryland development. *Science* **316**: 847–851, DOI: 10.1126/science.1131634.

Schlesinger WH, Reynolds JF, Cunningham GL, Huenneke LF, Jarrell WM, Virginia RA, Whitford WG. 1990. Biological feedbacks in global desertification. *Science* **247**: 1043–1048.

Sun H, Pan Z, Liu X. 2012. Numerical simulation of spatial-temporal distribution of dust aerosol and its direct radiative effects on East Asian climate. *J. Geophys. Res.* **117**(D13206), DOI: 10.1029/2011JD017219.

UNEP. 1992. *World Atlas of Desertification*. Edward Arnold: London.

Van der Werf GR, Randerson JT, Collatz GJ, Giglio L, Kasibhatla PS, Arellano AF, Olsen SC, Kasischke ES. 2004. Continental-scale partitioning of fire emissions during the 1997 to 2001 El Nino/La Nina period. *Science* **303**: 73–76.

Wiscombe WJ. 1980. Improved Mie scattering algorithms. *Appl. Opt.* **19**: 1505–1509.

Wu T, Yu R, Zhang F. 2010. The Beijing Climate Center atmospheric general circulation model: description and its performance for the present-day climate. *Clim. Dyn.* **34**: 123–147, DOI: 10.1007/s00382-008-0487-2.

Wei X, Zhang H. 2011. Analysis of optical properties of non-spherical dust aerosols. *Acta. Opt. Sin.* **31**(5): 0501002 (in Chinese).

Wang Z, Zhang H, Jing X, Wei X. 2013. Effect of non-spherical dust aerosol on its direct radiative forcing. *Atmos. Res.* **120**: 112–126, DOI: 10.1016/j.atmosres.2012.08.006.

Zender CS, Bian H, Newman D. 2003. The mineral dust entrainment and deposition (DEAD) model: description and 1990s dust climatology. *J. Geophys. Res.* **108**(D14): 4416, DOI: 10.1029/2002JD002775.

Zhang H, Nakajima T, Shi G. 2003a. An optical approach to overlapping bands with correlated *k* distribution method and its application to radiative calculations. *J. Geophys. Res.* **108**(D20): 4641, DOI: 10.1029/2002JD003358.

Zhang XY, Gong SL, Shen ZX, Mei FM, Xi XX, Liu LC, Zhou ZJ, Wang D, Wang YQ, Cheng Y. 2003b. Characterization of soil dust aerosol in China and its transport and distribution during 2001 ACE-Asia: 1. Network observations. *J. Geophys. Res.* **108**(D9): 4261, DOI: 10.1029/2002JD002632.

Zhang H, Suzuki T, Nakajima T, Shi G, Zhang X, Liu Y. 2006a. Effects of band division on radiative calculations. *Opt. Eng.* **45**(1): 016002, DOI: 10.1117/1.2160521.

Zhang H, Shi G, Nakajima T, Suzuki T. 2006b. The effects of the choice of the *k*-interval number on radiative calculations. *J. Quant. Spectrosc. Radiat. Transf.* **98**(1): 31–43, DOI: 10.1016/j.jqsrt.2005.05.090.

Zhang H, Wang Z, Wang Z, Liu Q, Gong S, Zhang X, Shen Z, Lu P, Wei X, Che H, Li L. 2012. Simulation of direct radiative forcing of aerosols and their effects on East Asian climate using an interactive AGCM-aerosol coupled system. *Clim. Dyn.* **38**: 1675–1693, DOI: 10.1007/s00382-011-1131-0.

Zhang H, Jing X, Li J. 2014. Application and evaluation of a new radiation code under McICA scheme in BCC_AGCM2.0.1. *Geosci. Model Dev.* **7**: 737–754, DOI: 10.5194/gmd-7-737-2014.

Zhou CH, Gong SL, Zhang XY, Liu HL, Xue M, Cao GL, An XQ, Che HZ, Zhang YM, Niu T. 2012. Towards the improvements of simulating the chemical and optical properties of Chinese aerosols using an online coupled model CUACE/Aero. *Tellus B.* **64**: 18965, DOI: 10.3402/tellusb.v64i0.18965.

Zhao C, Liu X, Leung LR. 2012. Impact of the desert dust on the summer monsoon system over southwestern North America. *Atmos. Chem. Phys.* **12**: 3717–3731, DOI: 10.5194/acp-12-3717-2012.

Zhao S, H Zhang, X Zhi, Z Wang, Z Wang. 2014. A primary assessment of the simulated climatic state by a coupled aerosol-climate model BCC_AGCM2.0.1_CAM. *Clim. Env. Res.* **19**(3): 265–277, DOI: 10.3878/j.issn.1006-9585.2012.12015 (in Chinese).

